LAWRENCE
LIVERMORE
NATIONAL
LABORATORY

LLNL-PROC-655361

Investigating high speed phenomena in laser plasma interactions using DIXI (DIlation X-ray Imager)

S. R. Nagel, T. J. Hilsabeck, P. M. Bell, D. K. Bradley, M. J. Ayers, K. Piston, B. Felker, J. D. Kilkenny, T. Chung, J. D. Hares, A. K. L. Dymoke-Bradshaw

June 4, 2014

20th Topical Conference on High-Temperature Plasma Diagnostics (HTPD 2014)
Atlanta, GA, United States
June 1, 2014 through June 5, 2014

Disclaimer

Investigating high speed phenomena in laser plasma interactions using DIXI (dilation x-ray imager)[a)]

S. R. Nagel,[1, b)] T. J. Hilsabeck,[2] P. M. Bell,[1] D. K. Bradley,[1] M.J. Ayers,[1] K. Piston,[1] B. Felker,[1] J. D. Kilkenny,[2] T. Chung,[2] B. Sammuli,[2] J. D. Hares,[3] and A. K. L. Dymoke-Bradshaw[3]
[1)] *Lawrence Livermore National Laboratory, 7000 East Avenue, Livermore, California 94550, USA*
[2)] *General Atomics, P.O. Box 85608, San Diego, California 92186-5608, USA*
[3)] *Kentech Instruments Ltd., Wallingford, Oxfordshire OX10, United Kingdom*

(Dated: 4 June 2014)

The DIlation X-ray Imager (DIXI) is a new, high-speed x-ray framing camera at the National Ignition Facility (NIF) sensitive to x-rays in the range of ≈2-17 keV. DIXI uses the pulse-dilation technique to achieve a temporal resolution of less than 10 ps, a ≈10× improvement over conventional framing cameras currently employed on the NIF (≈100 ps resolution), and otherwise only attainable with 1D streaked imaging. The pulse-dilation technique utilizes a voltage ramp to impart a velocity gradient on the signal-bearing electrons. The temporal response, spatial resolution and x-ray sensitivity of DIXI are characterized with a short x-ray impulse generated using the COMET laser facility at LLNL. At the NIF a pinhole array at 10 cm from target chamber center (tcc) projects images onto the photocathode situated outside the NIF chamber wall with a magnification of ≈64×. DIXI will provide important capabilities for warm-dense-matter physics, high-energy-density science and inertial confinement fusion, adding important capabilities to temporally resolve hot-spot formation, x-ray emission, fuel motion and mix levels in the hot-spot at neutron yields of up to 10^{17}. We present characterization data as well as first results on electron-transport phenomena in buried-layer foil experiments.

I. INTRODUCTION

At the NIF gated imagers are currently used to image the shape of implosions and measure the peak x-ray emission in order to improve the performance of the implosions.[1–3] The images are obtained using pinhole imaging, where an array of pinholes throws an array of images onto the detector. To achieve temporal resolution the detectors used are gated microchannel plates (mcp). These are the current state-of-the-art detectors that have been around for decades. Temporal gating of the signal is achieved by sending a fast voltage pulse along a gold coating on the mcp. The voltage pulse generates the gain of the signal[4]. The electron transit time spread through the mcp pores however limits the temporal resolution of these detectors. Therefore to achieve shorter gate times the thickness of the plates would have to be reduced. However, going to thinner plates is impractical, as it leads to lower gain and the transmission of x-rays directly onto the phosphor/detector. The temporal resolution of these mcp based detectors is therefore limited to 35-100 ps[4]. A different technology is needed to achieve gate times of < 30 ps.

Obtaining better understanding of ICF motivates the improvement of gate times to < 30 ps. There are many other possible applications for faster x-ray cameras to investigate ultra-fast phenomena such as fast electron transport in short pulse laser-plasma interactions.

Here we will show that the pulse dilation principle, discussed in[5], has successfully been implemented into a new generation of gated x-ray imagers with measured temporal resolution of down to 5 ps. DIXI (DIlation X-ray Imager) was designed to record 2D x-ray images with high temporal resolution in a hostile, high neutron environment such as the National Ignition Facility (NIF). It will look at the imploding core and work on improving its performance.

II. INSTRUMENT DESCRIPTION

To achieve its high temporal resolution, DIXI utilizes the concept of pulse-dilation, or stretching of the signal. In short the pulse-dilation technique uses a voltage ramp

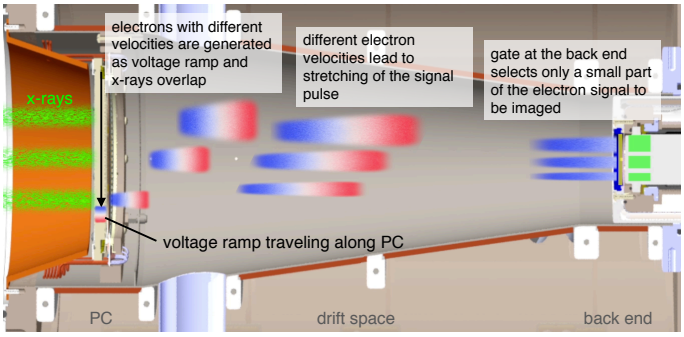

FIG. 1. DIXI working principle

[a)] Invited paper published as part of the Proceedings of the 20th Topical Conference on High-Temperature Plasma Diagnostics, Atlanta, Georgia, June, 2014.
[b)] Author to whom correspondence should be addressed: nagel7@llnl.gov.

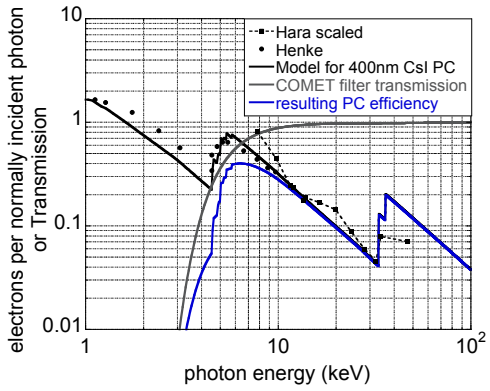

FIG. 2. Spectral sensitivity of the CsI photocathode, following Henke[6]. This is convolved with the filter transmission to obtain the resulting PC efficiency.

to impart a velocity gradient on the signal-bearing electrons that are generated when x-rays hit the transmission photocathode (PC)[6].

Figure 1 shows the working principle of the instrument. The PC converts the incoming x-ray signal into electrons. Because the PC is pulsed by a voltage ramp, the generated electrons have energies that depend on the time and space at which they were born. The resultant effect is that the electrons generated by an earlier part of the signal travel faster than the ones generated by the part of the signal that arrives later in time. As the electrons travel to the recording medium, the signal is stretched or dilated. In the current instrument design, the signal arriving at the detector is on the order of 50 times longer than the initial one, see equation 2. This stretched out signal now allows us to use a standard gated detector in the back of the instrument to look only at a small part of the 50-times-longer signal. The back end consists of a single strip gated mcp detector, followed by a phosphor, fiber block and a ccd/film back. As an example, using a 500 ps gate at the back gives a temporal resolution of 10 ps.

The time at which the electrons exit the drift region or reach the back of the drift space is dependent on the time at which the electrons enter the drift region, t_i, and is given by

$$t_i' = L\sqrt{\frac{m_e}{2\,e\,\Phi(t_i)}} + t_i. \tag{1}$$

The temporal magnification M between two time steps is:

$$M(t_1, t_0) = \frac{t_1' - t_0'}{t_1 - t_0} \approx 1 + \frac{L}{2v_d}\frac{|\dot{\Phi}|}{\Phi}, \tag{2}$$

where v_d is the drift velocity of the electron

$$v_d = \sqrt{\frac{2e\Phi(x,t)}{m_e}} \tag{3}$$

Therefore the effective instrument gate width, gw, is given by

$$gw = \frac{t_{\rm mcp}}{M}. \tag{4}$$

Table I lists the values relevant for the current DIXI design. Figure 5 shows the calculated gate widths (solid line) for different PC bias voltages.

As can be seen from equations 2-4 there are four parameters that determine the effective shutter speed of DIXI. The first parameter is the PC bias voltage, $\Phi(t = 0)$, which determines the mean velocity of the electrons and therefore how long they spend in the drift space. The second parameter is the gradient of the fast PC voltage ramp, $|\dot{\Phi}|$, which determines the electron dispersion. The third parameter is the length of the drift tube, L, which influences the time available for the pulse dilation and the fourth parameter is the mcp gate width at the back of the drift space, $t_{\rm mcp}$. This determines how much of the dilated electron signal is detected.

To get a more accurate idea of the limitation on the gate width the finite accelerating gap and finite temperature, T_e, have to be taken into account. Simulations have been run to gauge the effects for a 1.6 mm gap and 1.7 eV photoelectron temperature on the gate width for different PC bias voltages, shown as the dashed line in figure 5. This show a roll over at low voltages mainly dominated by the finite temperature.

Because the voltage ramp that travels along the PC acts like a traveling shutter, the result without an imaging optic in front of DIXI resembles that of a streak camera, in that along the length of the PC only temporal information can be obtained. However, in contrast to a streak camera, by placing a pinhole (PH) or PH array between the x-ray source and DIXI, we can obtain multiple 2D images along the length of the PC. Then the images at the beginning of the strip are captured earlier in time

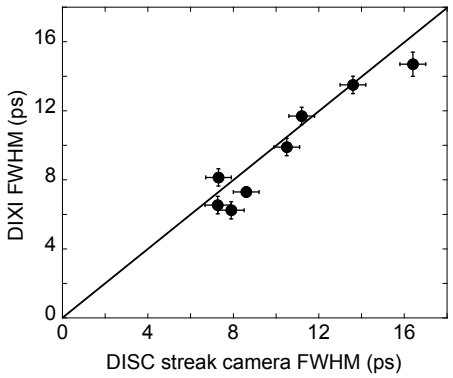

FIG. 3. Temporal response comparison between DIXI and and x-ray streak camera (DISC). DIXI provides 2D x-ray imaging with temporal resolution currently only achievable with 1D streak cameras. For the very short impulses the measurement appears to have been source width limited.

TABLE I. Values for DIXI gate time calculations.

Quantity	value	unit
$\lvert\dot{\Phi}\rvert$	5	V/ps
L	486	mm
$t_{\rm mcp}$	450	ps
$\Phi(t=0)$	PC bias	V
Cathode to Anode	1.6	mm

than the ones at the end of the strip. The gating of the strip allows the x-ray images to be captured at different times, enabling a reconstruction of the target shape size and burn history.

The spectral sensitivity of the CsI PC is modeled using Henke[6], and can be seen in figure 2. The figure also shows the transmission of the filter setup used in the COMET characterization and the resulting effective efficiency of the PC.

As described in[7], the spatial resolution of DIXI depends on the PC material as well as the magnetic field strength at the PC. This is reproduced in figure 7. The spatial resolution of the instrument, $\delta_{\rm instr}$, is determined by the spatial resolution of the PC itself $\delta_{\rm PC}$ and the MCP detector $\delta_{\rm mcp}$.

$$\delta_{\rm instr} = \sqrt{\delta_{\rm PC}^2 + (\delta_{\rm mcp} \times {\rm Mag}_B)^2} \qquad (5)$$

The spatial resolution of the gated MCP detector is 45 μm, but because of the de-magnification by the magnetic field translates to ${\rm Mag}_B \times \delta_{\rm mcp} \approx 2.5{\times}45$ μm at the PC. ${\rm Mag}_B$ depends on the magnetic field within the vessel. $\delta_{\rm PC}$ depends on the material of the PC and the magnetic field strength at its position. This is because secondary photoelectrons are ejected with a characteristic energy spread depending on the PC material. Here we compare CsI and Au as the active PC materials. CsI has

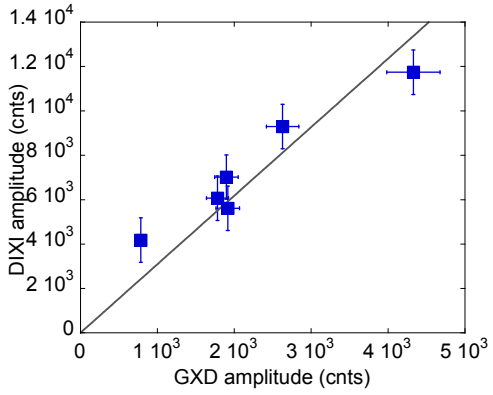

FIG. 4. Comparison between the peak signal levels measured by DIXI and the ones measure by an mcp based framing camera (gated x-ray detector, GXD). A linear correlation in the non-saturated regime is observed.

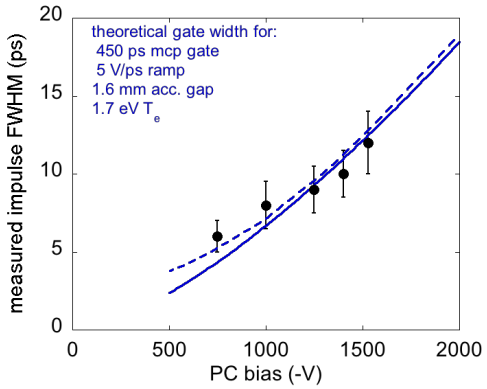

FIG. 5. The measured gate width for different PC bias voltage settings agrees well with the expected dependence. The dashed line shows the simulated gate width for an acceleration gap of 1.6 mm and an electron temperature T_e=1.7 eV. The solid line shows the gate width, gw, calculated using equations 2-4.

two distinct advantages over Au, namely it gives a better spatial resolution and also has a higher sensitivity, that is more secondary electrons are generated per incident photon. CsI has a characteristic energy spread of 1.7 eV, compared to Au at 3.5 eV[6]. In the solenoid field the transverse excursion of the photoelectrons, and therefore $\delta_{\rm PC}$, is limited to 4 times their cyclotron radius[5].

$$\delta_{\rm PC} = 4r_L[\mu m] = 95000\frac{\sqrt{T_e[eV]}}{B[{\rm Gauss}]}. \qquad (6)$$

This shows that the spatial resolution is inversely proportional to the magnetic field at the PC. The resulting theoretical instrument resolution using equations 5 and 6 is plotted in figure 7 (solid lines) for different magnetic fields at the PC and the two PC materials. For the data in this paper DIXI was always run with a CsI PC and a magnetic field strength at the PC of 500 Gauss.

III. INSTRUMENT CHARACTERIZATION MEASUREMENTS

The instrument characterization measurements were taken using the COMET laser. COMET is part of the Jupiter Laser Facility (JLF) at LLNL. The laser had a pulse duration of $\approx$ 500-800 fs, a wavelength fo 1.054 μm and a spot size of FWHM $\approx$ 8 μm. This lead to intensities of $\approx 2\ 10^{19}$ Wcm^{-2}. The laser was focused onto a solid target, usually Cu or Zr foils. The generated x-rays had an unobstructed path to the instrument, which was run in pulsed mode. An example image and outline can be seen in reference[7] (fig. 4). Note that the FWHM of the gaussian fitted to the line outs to determine the signal width is biased to the rise of the signal. This gives a more accurate measurement of the effective gate width

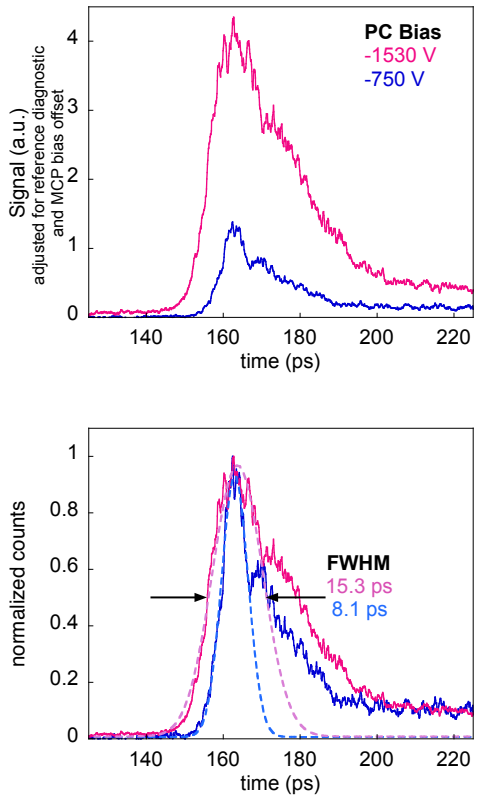

FIG. 6. (top) A significant reduction in signal level can be seen for a reduced bias voltage (shorter gate times). (bottom) The PC bias voltage at the PC is one of the parameters that determines the effective gate of the instrument. This can be seen when the curves are normalized to the peak value

as the falling edge of the signal is widened by plasma effects.

The temporal resolution of DIXI is measured and compared to simultaneous streak camera measurements. The result can be seen in figure 3. The temporal width of the source was changed to obtain this data, and the temporal profile measurements from the two instruments are in good agreement. This shows that DIXI can provide 2D x-ray imaging with a temporal resolution that is currently only achievable with 1D streak cameras. Figure 7 also shows comparison measurements between DIXI and the Gated X-ray Detector (GXD), which is an mcp based x-ray imager. Here the measured peak value of the emission is compared for the two gated detectors. This shows a linear dependency with currently used gated detectors.

In Section II it was shown that the gate width of DIXI depends on the PC bias voltage, $\Phi(t=0)$, or in other words the mean electron drift velocity. While keeping the source duration constant, a scan of the PC bias voltage was conducted. This can be seen in figure 5. Here the back end gate width was 400-450 ps and the voltage ramp, $|\dot{\Phi}|$, was 5 V/ps. The lowest gate widths seem to be limited by the source width and shot to shot reproducibility.

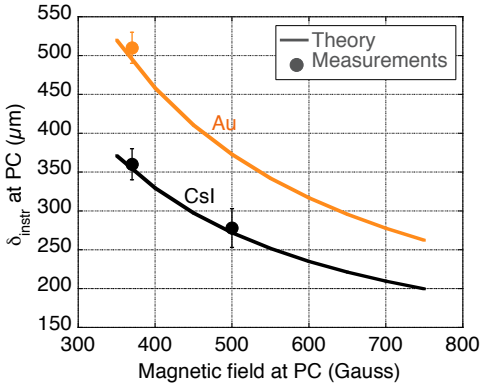

FIG. 7. Instrument resolution ($\delta_{\rm instr}$) at the PC plotted against magnetic field strength at the PC for two different PC materials (Au and CsI). The solid symbols show the experimentally measured (10-90% rise) spatial resolutions.

Figure 5 shows that because of the way that DIXI works, we can easily adjust the effective gate time of DIXI. However, reducing the gate width also reduces the collected signal. This can be seen in figure 6. The reason for the reduced signal for a shorter gate width is the increased temporal magnification, as the electron signal takes longer to traverse the drift space, and with the same velocity gradient, this leads to a more dilated signal. The signal level increases by $\approx 3\times$ for the increase from 750V to 1530V in PC bias voltage. This agrees well with the expected value of $M(\Phi = 1530)/M(\Phi = 750) \approx 2.9$. The figure on the bottom of figure 6 shows the curves normalized to the peak value and illustrates the broadening of the signal due to the change in gate width. Note that the shots in figure 6 were taken with a different mcp than the data in figure 5.

The spatial resolution measurements for the CsI PC, also discussed in[7], were extended to a higher magnetic field setting at the PC to an extraction field of 500 Gauss. The measurements of the 10-90% rise, seen in figure 7, are in good agreement with the theory described in section II and the spatial resolution of $<$ 300 μm satisfies the NIF requirement for the overall spatial resolution of the images to not be instrument limited. The spatial resolution can be further improved by increasing the magnetic field at the PC even more.

IV. INSTRUMENT SETUP AT THE NIF

At the NIF DIXI is situated on the equatorial plane outside the target chamber (port 90/100). The back end of DIXI is tilted down by 20 degrees from the horizontal plane, see figure 8. This shields the mcp detector from the direct line of sight and enhances the shielding of the ccd camera. As the strip orientation on the PC is vertical, the tilt angle of the instrument changes

the effective speed of the high voltage pulse along the PC. This is illustrated in fig. 8 (bottom). The time delay for an x-ray signal striking the photocathode between points A and B is $t_x(x') = \frac{x' \sin\theta}{c}$. The time it takes for the voltage ramp to move from A to B is $t_v(x') = \frac{x'}{v}$. The effective gate time across the image plane is given by $t_{\rm gate}(x') = t_x(x') + t_v(x') = x'(\frac{\sin\theta}{c} + \frac{1}{v})$, and the effective gate time across the object plane is given by $t_{\rm obj}(x) = t_x(x) + t_v(x) = x(\frac{\tan\theta}{c} + \frac{1}{v\cos\theta})$, using $x = x'\cos\theta$ and $y = x'\sin\theta$. The resulting change in the time delay along the strip is listed in table II.

With the currently used large magnification of 64×, the resulting images at the PC are large. As the gate times of DIXI are very fast, we now have to take into account that such large images might have a temporal difference from one side of the image to the other. For example, an emission diameter of 60 μm with a magnification of 64× leads to a diameter of 3.84 mm at the PC. Taking into account the tilt in the time direction of DIXI, this leads to a diameter in the time direction of 4.09 mm. Therefore the top of the image on the strips is [(4.09 mm)*(0.0805 ps/pix)/(22.47 μm/pix)= (3.84 mm)*(0.0805 ps/pix)/(21.11 μm/pix)]=14.6 ps earlier than the bottom of the image. To enhance the temporal resolution for larger images, two images separated in time by 10 ps can be used to obtain a shorter gate time across the image. These images can either be on the same strip, separated in the time direction if the PH array allows, or on two different strips that are timed so that half of one image is taken at the same time as the other half of another image to construct one image taken at the same time. To be able to use the latter method

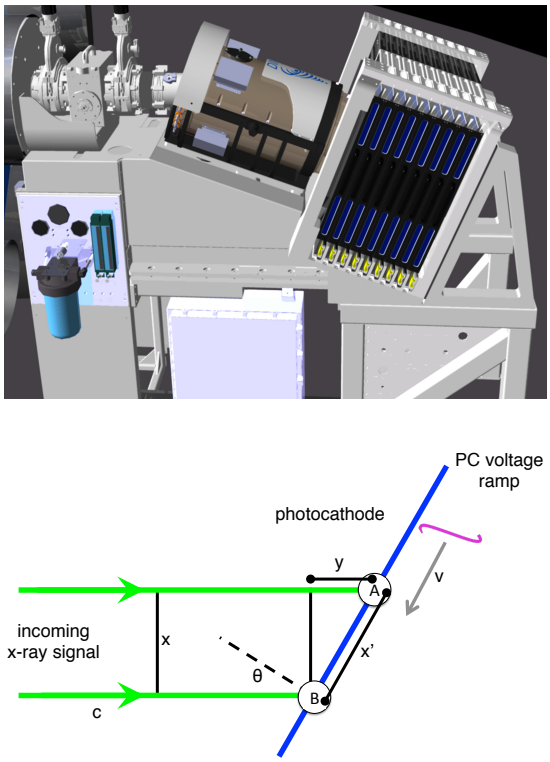

FIG. 8. (top) View of DIXI sitting outside the NIF target chamber with the back end of the instrument tilted off the direct line of sight, allowing for extra shielding. (bottom) Schematic of the tilted PC and the implementation on the effective shutter speed.

TABLE II. Values relevant for temporal conversion for a voltage setting of the magnetic coils of (785 (mcp), 785 (center-back), 715 (center-front), 815 (PC)), corresponding to 500 Gauss at the PC and an internal instrument demagnification of 2.5x. 1pixel is 9 μm x 9 μm. (*)measured independently with UV $v = 0.98\ c$.

DIXI orientation	Straight	$\theta = 20°$	units
v of voltage ramp along PC(*)	279	279	μm/ps
PC temporal conversion	0.0805		ps/pix
spatial magnification up/down	22.47	21.11	μm/pix
spatial magnification left/right	22.47	22.47	μm/pix

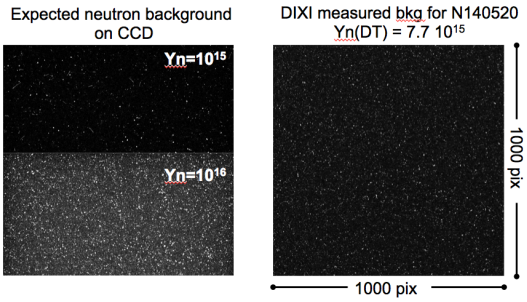

FIG. 9. Expected neutron induced background for two neutron yields compared to an actual background taken at Y_n ≈7.7 10^{15}. This shows that the measured background agrees with the expected levels.

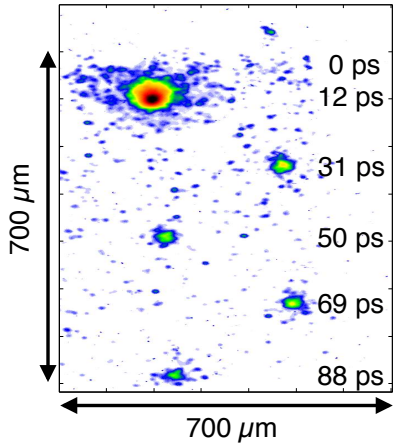

FIG. 10. Example of DIXI data taken on a TITAN experiment. The data shows the temporal evolution of the x-ray spot taken on a single shot.

for larger field of views, the jitter between strips has to be < 2 ps. This has been described and measured in[7].

The instrument is installed at NIF, and first neutron background measurements, see figure 9, show good agreement with predictions of the neutron induced background on the ccd for relevant yields.

V. TIME RESOLVED 2D X-RAY EMISSION DATA

Recently DIXI has participated on a physics experiment at the TITAN laser investigating high speed electron transport phenomena. A section of an example image illustrating the temporal evolution of the x-ray spot taken on a single shot can be seen in figure 10. The analysis and physics interpretation of the data is in preparation for publication.

VI. SUMMARY

In summary we have shown that DIXI has variable temporal resolution that can achieve gate times between 5-30 ps using the pulse dilation principle. DIXI provides 2D x-ray imaging with temporal resolution currently only achievable with 1D streak cameras. Such a fast gate time means that for large images one has to worry about the timing changing from one side of the image to the other. The characterization measurement agree well with the predicted behavior of the instrument and DIXI is on its way to add important capabilities to temporally resolve hot-spot formation, x-ray emission, fuel motion and mix levels in the hot-spot at neutron yields of up to 10^{17}.

ACKNOWLEDGMENTS

The Authors would like to acknowledge the support of the staff at the Jupiter Laser Facility and thank the Shape Group or providing the modeling results. Lawrence Livermore National Laboratory is operated by Lawrence Livermore National Security, LLC, for the U.S. Department of Energy, National Nuclear Security Administration under Contract No. DE-AC52-07NA27344. (LLNL-PROC-655361)

[1] S. Atzeni and J. Meyer-ter Vehn, The Physics of Inertial Fusion, International Series of Monographs on Physics (Clarendon Press, Oxford, 2004); J. D. Lindl, Inertial Confinement Fusion: The Quest for Ignition and Energy Gain Using Indirect Drive (Springer-Verlag, New York, 1998).

[2] J. R. Rygg, O. S. Jones, J. E. Field, M. A. Barrios, L. R. Benedetti, G. W. Collins, D. C. Eder, M. J. Edwards, J. L. Kline, J. J. Kroll, O. L. Landen, T. Ma, A. Pak, J. L. Peterson, K. Raman, R. P. J. Town, and D. K. Bradley, Physical Review Letters 112, 195001 (2014).

[3] R. P. J. Town, D. K. Bradley, A. Kritcher, O. S. Jones, J. R. Rygg, R. Tommasini, M. Barrios, L. R. Benedetti, L. F. Berzak Hopkins, P. M. Celliers, T. Döppner, E. L. Dewald, D. C. Eder, J. E. Field, S. M. Glenn, N. Izumi, S. W. Haan, S. F. Khan, J. L. Kline, G. A. Kyrala, T. Ma, J. L. Milovich, J. D. Moody, S. R. Nagel, A. Pak, J. L. Peterson, H. F. Robey, J. S. Ross, R. H. H. Scott, B. K. Spears, M. J. Edwards, J. D. Kilkenny, and O. L. Landen, Physics of Plasmas 21, 056313 (2014)

[4] D. K. Bradley, P. M. Bell, O. L. Landen, J. D. Kilkenny, and J. Oertel, Rev. Sci. Instrum. 66, 716 (1995).

[5] T. J. Hilsabeck et al., Rev. of Sci. Instrum., 81, 10E317 (2010).

[6] B. L. Henke, J. P. Knauer and K. Premaratne, J. Appl. Phys. 52(3), 1509 (1981).

[7] S. R. Nagel et al., Rev. of Sci. Instrum., 83, 10E116 (2012).